Study on Linear Density Effect on the Vibration Behavior of Textile Strings Using Video Processing

Mina Emadi, Pedram Payvandy*, Mohammad Ali Tavanaie, and Mohammad Mahdi Jalili

Abstract- **The main aim of this study is to obtain a detailed information about textile string vibration and the effect of physical properties changes on it. This is based on the fact that modal parameters are the functions of physical properties. Video cameras propose the unique capability of collecting high density spatial data from a distant view and supply a reliable method for measuring vibrations and displacements in structures. They could be employed as inspection sensors because of their normal use, ease, and low cost. In this research, some laboratory equipment with a high-speed digital camera was designed to measure the vibration behavior of polypropylene monofilaments. The vibration was recorded by the high-speed camera at all the points of the string, and video processing was done to extract the free decays. The natural frequency, amplitude and phase were obtained by the Fourier series. The logarithmic decrement and the damping coefficient for monofilaments were calculated. The experimental results were compared to the results of a theoretical model for a plucked string with viscous damping, and the vibration properties of monofilaments were obtained. As the results showed, the theoretical model could successfully predict the vibration behavior of the filaments with error less than 23%. The trend of changes in the monofilament physical properties was easily specified based on the trend of the variations in the damping coefficient and the natural frequency. It was found that an increase in the monofilament linear density would cause a decrease in the damping coefficient and its natural frequency.**

Keywords: **vibration analysis, monofilament, high-speed camera, computer vision**

M. Emadi and P. Payvandy
Textile Engineering Department, Yazd University, Yazd, Iran; and Center of Excellence for Machine Vision in Textile and Apparel Industry, Yazd University, Yazd, Iran.

M.A. Tavanaie
Textile Engineering Department, Amirkabir University of Technology, Tehran, Iran; and Center of Excellence for Machine Vision in Textile and Apparel Industry, Yazd University, Yazd, Iran.

M.M. Jalili
Mechanical Engineering Department, Yazd University, Yazd, Iran.

Correspondence should be addressed to P. Payvandy
e-mail: peivandi@yazd.ac.ir

I. INTRODUCTION

A large bulk of the literature on textiles has been dedicated to the identification of the physical and apparent properties of textile strings (e.g. yarns, multifilaments, and monofilaments). The vibration behavior of a string can be used as a parameter to identify its physical and apparent properties. Some measuring instruments determine the physical properties of fibers based on the vibration method and using optoelectronic sensors. This is based on the idea that modal parameters, notably frequencies, mode shapes, and modal damping, are the functions of such physical properties as mass, damping, and stiffness.

There are many different contact methods to carry out experiments on string vibrations. Sometimes, however, the special characteristics of a structure call for a certain non-contact method. Non-contact vibration measurement methods can be divided into three categories including electromagnetic methods [1], use of electrical sensors [2], and optical methods. The major problem with electromagnetic and electric methods is that they work only for conducting (metal) strings and may influence the strings motion by damping them. Besides, these methods need extensive calibration. Optical methods are able to provide a wide range of vibration information for structures. In these methods, high-speed cameras [3-7] and techniques such as digital image processing [8-10] can be used successfully to measure string vibration.

There is little research on vibration in textile strings. In a study by Gao *et al.* [11], the transversal vibration of a pile-yarn with time-dependent tension in the tufting process was examined. The pile-yarn was modeled as Kelvin-Voigt elements, and the effects of the transport speed, the tension perturbation amplitude and the damping coefficient on its vibration behavior were studied numerically. The results of the numerical studies showed that, once the damping coefficient is increased and the range of stress fluctuation is decreased, it is possible to control the vibration of the yarn in a tufting process. In another study by Gao *et al.* [12], an analysis was conducted of the mechanical behavior of carpet yarns by standard linear and nonlinear viscoelastic

models. These models were used to simulate the tensile properties, stress and creep behavior of yarns. The obtained formulas were fitted with experimental data. As the results indicated, the standard linear model fitted well with the tensile, relaxation and creep experimental curves and could be employed to analyze the vibration properties of yarns during the weaving process.

Shen *et al.* [13] studied the dynamic characteristics of warps in the weaving process. Through numerical analyses, they evaluated the effects of different parameters such as viscosity, damping coefficient, warp velocity, and tensile fluctuations on the dynamic response of warps. Flexural rigidity, torsional stiffness and shear stiffness were not taken into account, and a simple Kelvin model was used to analyze the vibration equation of the warps. It was shown that, for some types of warps, the frequency of vibration is related to their velocity, their length, and the amplitude of stress fluctuation. Malookani *et al.* [14] studied the transversal vibrations of an axially moving string under boundary damping. The asymptotic approximations for the solution of the equations were obtained by two time-scale perturbation and the characteristic coordinates methods. The vertical displacement of the moving string was calculated by using specific initial conditions. It has been shown how the damping at the boundary may affect the vertical displacement of the axial system. In the study by Serrano *et al.* [15] the dynamic behavior of a stretched string modeled as a lattice of particles linked to first neighbors by linear springs was studied. In this work an inertia-gradient generalized continuum model of the chain, which undergoes nonlinear vibrations was developed. Zhang *et al.* [16] focused on the modelling of a tightly stretched nano-string with elastically supported ends by the central finite difference model, the lattice model and the Eringen's nonlocal model. The analytical vibration solutions for lattice model were obtained by solving the linear second-order finite difference equation. Ferretti *et al.* [17] studied the nonlinear dynamics of a horizontal, initially taut and elastic string. A kinematic nonlinear model for the free boundary problem was resumed. The dynamic tension was accounted in the equations of motion, as a nonlinear effect. The simplified equations were discretized by the Galerkin method and numerical results were obtained.

In the above-mentioned studies, one rarely comes across any account of how the physical and apparent properties of a string affect its vibration behavior. Nowadays, the study of the wide range of fiber properties is necessary for quality control purposes in fiber production and for evaluating the process ability of fibers in spinning. The purpose of this study is to investigate the vibration behavior of monofilaments as a procedure for identifying their physical and apparent properties using high-speed camera and video processing. It also serves as a non-destructive, reliable and effective procedure for the quality control of textile strings. The vibration of a string at all of its points was recorded by a high-speed camera, and video processing was done to extract the free decays. The Fourier transform method and logarithmic decrement were used to analyze the signals, and the experimental results were compared to a theoretical model for plucked strings with viscous damping.

A. Modal Analysis of the Tight String

A.1. Vibration Theory of the Plucked Strings

Let's have a string with the length of L, density of ρ(x) per unit length, and fixed ends as shown in Fig. 1. The equation of vibration motion becomes:

$$\frac{\partial}{\partial x}\left(\tau(x)\frac{\partial u}{\partial x}\right)+f(x,t)=\rho(x)\frac{\partial^2 u}{\partial t^2} \tag{1}$$

Eq. (1) is the general equation of the wave where linear density ρ and tension τ are the functions of the position (x) and f(x,t) is also the external force. It should be noted that a free vibration with a constant linear density and tension was used in this study. Using Newton's second law and the variables separation method, the general solution for the transverse vibrational motion of this string, is obtained as follows:

$$u(x,t)=\sum_{n=1}^{\infty}\left(A_n\cos\omega_n t+B_n\sin\omega_n t\right)\sin\frac{n\pi}{L}x \tag{2}$$

Where, $c=(\tau/\rho)^{0.5}$ is the speed of propagation of the wave and $\omega_n=n\pi c/L$ is the natural frequency. The unknown constants A_n and B_n also occur discretely, and they must be determined by using the initial conditions and applying the principle of orthogonality of modes. Consider the following example of a plucked string (Fig. 2) with initial

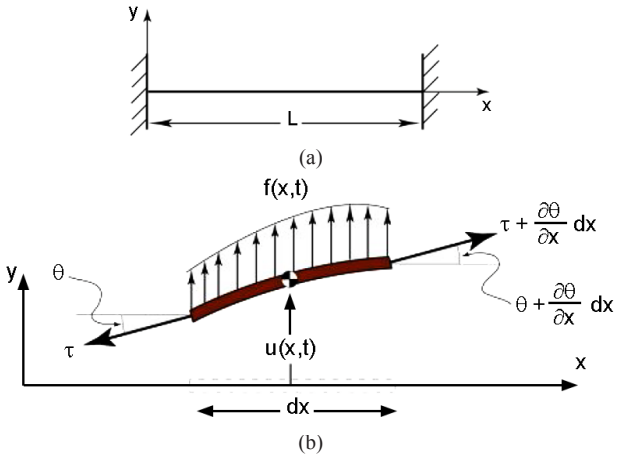

Fig. 1. (a) Geometry of a tight string with fixed ends and (b) free body diagram of string element.

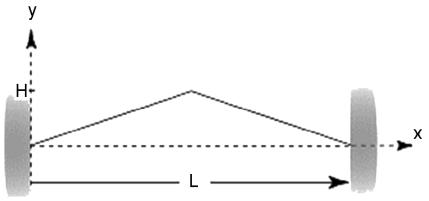

Fig. 2. Initial shape of a plucked string.

conditions given by:

$$u(x,0)=\begin{cases}\dfrac{2Hx}{L}, & 0\le x\le\dfrac{L}{2}\\ 2H\left(1-\dfrac{x}{L}\right), & \dfrac{L}{2}\le x\le L\end{cases}$$

and

$$\dot{u}(x,0)=0 \tag{3}$$

The equation coefficients A_n and B_n are determined and thus the total solution for transverse vibration motion of this string is written as follows:

$$u(x,t)=\frac{8H}{\pi^2}\sum_{n=1,3,5}^{\infty}\frac{1}{\pi^2}(-1)^{\frac{n-1}{2}}\sin\frac{n\pi}{L}x\cos\omega_n t \tag{4}$$

A.2. Effect of Damping on the Response of the Plucked String

The equation of motion tight string with constant tension and density, but including distributed damping is written as:

$$\rho\frac{\partial^2 u}{\partial t^2}+\beta\frac{\partial u}{\partial t}-\tau\frac{\partial^2 u}{\partial x^2}=f(x,t) \tag{5}$$

Where, β is the distributed viscous damping constant with units N.s/m^2. Hence, the general solution is given by:

$$u(x,t)=\sum_{n=1}^{\infty}\left(e^{-\zeta_n\omega_n t}(A_n\cos\omega_d t+B_n\sin\omega_d t)\right)\sin\frac{n\pi}{L}x \tag{6}$$

Where, $\zeta_n=\beta/(2\rho\omega_n)$ and $\omega_d=\omega_n(1-\zeta_n^2)^{0.5}$. The equation coefficients A_n and B_n are determined and thus the total solution for transverse vibration motion of this string can be written as follows [18] :

$$u(x,t)=\sum_{n=0}^{\infty}\left\{\frac{8H}{\pi^2}\frac{(-1)^n}{(2n+1)^2}\left(e^{-\zeta_n\omega_n t}\left(\cos\omega_d t+\frac{\zeta_n}{\sqrt{1-\zeta_n^2}}\sin\omega_d t\right)\right)\sin\frac{(2n+1)\pi}{L}x\right\} \tag{7}$$

A.3. Logarithmic Decrement

A convenient way of determining the damping in a system is to measure the rate of decay of oscillation. A larger damping, the greater will be the rate of decay. Consider a damped vibration expressed by the Eq. (8) and is shown in Fig. 3:

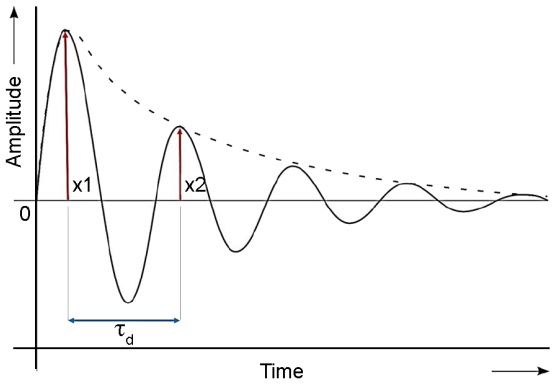

Fig. 3. Rate of decay of oscillation measured by the logarithmic decrement.

$$x=Xe^{-\zeta\omega_n t}\sin\left(\sqrt{1-\zeta^2}\omega_n t+\varphi\right) \tag{8}$$

The logarithmic decrement, δ is the natural logarithm of the ratio of any two successive amplitudes. The expression for the logarithmic decrement then becomes:

$$\delta=\ln\frac{x_1}{x_2}=\ln\frac{e^{-\zeta\omega_n t_1}\sin\left(\sqrt{1-\zeta^2}\omega_n t_1+\varphi\right)}{e^{-\zeta\omega_n(t_1+\tau_d)}\sin\left(\sqrt{1-\zeta^2}\omega_n(t_1+\tau_d)+\varphi\right)} \tag{9}$$

The values of the sins are equal when the time is increased by the damped period τ_d, the preceding relation is reduced to:

$$\delta=\ln\frac{e^{-\zeta\omega_n t_1}}{e^{-\zeta\omega_n(t_1+\tau_d)}}=\zeta\omega_n\tau_d \tag{10}$$

By substituting for the damped period $\tau_d=2\pi/\omega_n(1-\zeta^2)^{0.5}$, the expression for the logarithmic decrement becomes:

$$\delta=\frac{2\pi\zeta}{\sqrt{1-\zeta^2}} \tag{11}$$

Where, ζ is the damping ratio. The logarithmic decrement is also given by the Eq. (12), where x_n represents the amplitude after n cycles have elapsed [19]:

$$\delta=\frac{1}{n}\ln\frac{x_0}{x_n} \tag{12}$$

II. EXPERIMENTAL

A. Materials

Four polypropylene monofilaments and three copper wires were used in this research. The polypropylene monofilaments were prepared from SABIC PP 512P with 25 g/10 min melt flow rate and produced by the Dynisco Laboratory Melting Equipment at Yazd University Laboratory. The extruder speed was about 12 rpm, and the distance between the spinneret and the collecting roller

TABLE I
PROPERTIES OF THE STRINGS

Sample code	Material	Diameter (mm)	Linear density (g/m)	Denier
P-120	Polypropylene	0.120 CV%: 3.50	0.0101 CV%: 9.90	90.9
P-170	Polypropylene	0.170 CV%: 4.35	0.0224 CV%: 7.09	201.6
P-220	Polypropylene	0.220 CV%: 8.25	0.0321 CV%: 11.05	288.9
P-290	Polypropylene	0.290 CV%: 4.91	0.0683 CV%: 5.23	614.7
C-80	Copper	0.080 CV%: 5.87	0.0597 CV%: 4.67	537.3
C-135	Copper	0.135 CV%: 13.79	0.0993 CV%: 11.25	893.7
C-200	Copper	0.200 CV%: 6.47	0.2590 CV%: 8.15	2331

was 22 cm. The speed of the collecting roller was the only variable factor in the production of the monofilaments, which resulted in four monofilaments with difference diameters in size. The properties of the strings are presented in Table I.

B. Experiment Setup

The experiment setup is shown in Fig. 4. A set of components was used to construct a laboratory system for measuring the string vibration. These components included two fixed holders at the two ends of a string, an electric lock with a needle placed in the middle that could be used to deviate and release the string for its initial stimulation, a specific weight for the string initial tension, a box for direct and constant lighting on the sample, LED tubes for lighting, a high-speed camera, polypropylene monofilaments, and a cable and a laptop to receive and process videos. It should be noted that a Sony RX10 II camera was also used in this research. It had a 1.0-type (13.2 mm × 8.8 mm) Exmor® RS CMOS sensor with 960 frames per second.

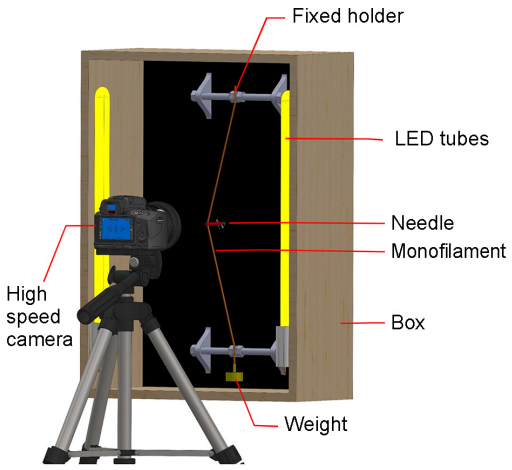

Fig. 4. A schematic display of the experimental setup.

C. Testing Method

The end of a 30 cm string was fixed in the upper holder and the other end was attached to a weight and released to form an initial tension in the string. Then, the bottom holder was fixed on the string to maintain this initial tension. The initial stimulation of the string was accomplished by a displacement in the middle of it. This stimulation occurred as the string was placed at the back of the needle and released at zero moments. The high-speed camera recorded the string vibrating motion which was then processed as a video file.

D. Optimization of the Test Conditions

Vibration tests were conducted for three copper wires (C-80, C-135, and C-200) to determine the optimal test parameters. The tension in the strings was provided by weights of 20, 50, and 100 g attached to the end of the strings. The initial stimulation was carried out by displacements of 4, 7, and 10 mm in the middle of the strings. Finally, the results of the video processing were examined to identify the best stimulation distance.

E. Extraction of the String Vibration Information

The video processing was conducted to extract the string free decays. As shown in the flowchart of Fig. 5, first, the video was read by the algorithm, and each video frame was saved as a color image. In order to track the string in vibration, one point of the string had to be selected and tracked across successive frames. A pixel bar was selected instead of one point. That pixel bar selected from the image

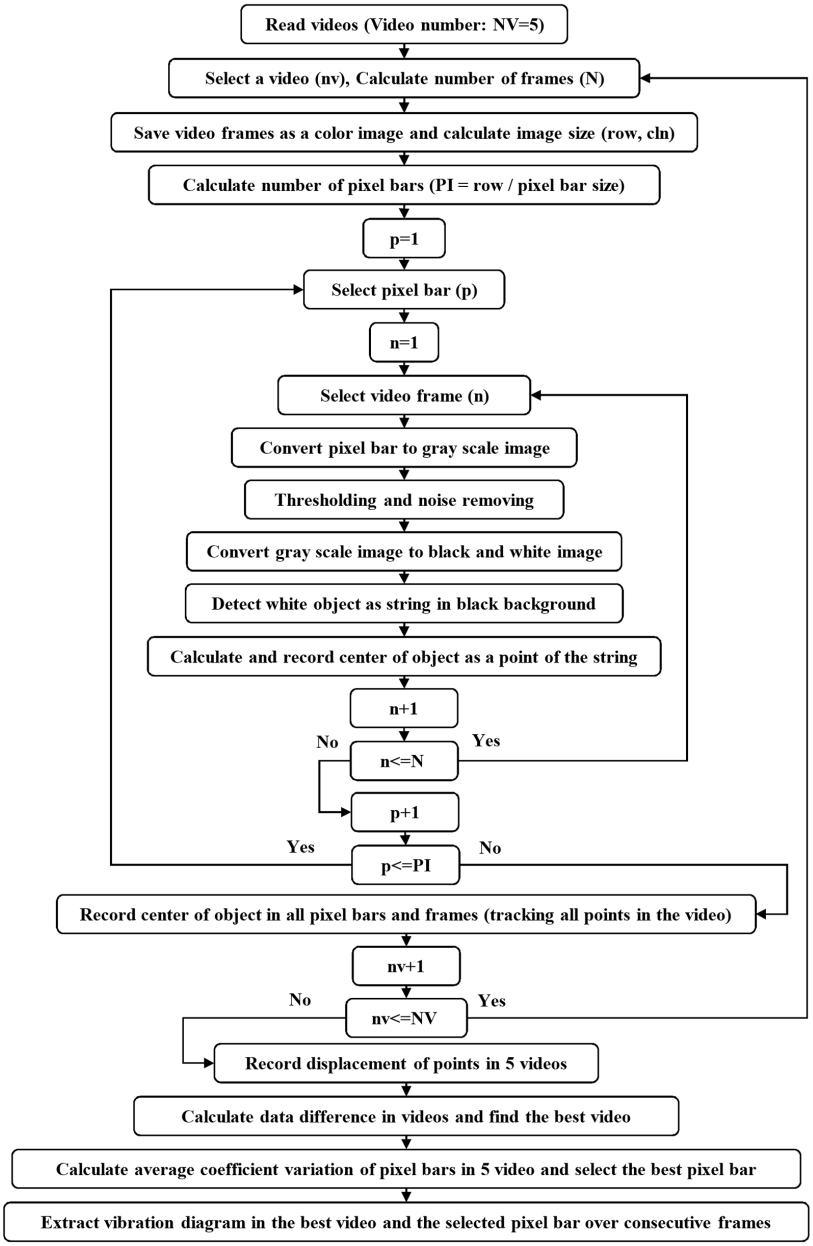

Fig. 5. Flowchart of the video processing.

was turned into a grayscale image, noises were removed, and then thresholding was done with the k-means algorithm to finally present a black and white image. In many studies, the k-means algorithm has been used as a suitable method to extract an object from the background of images [20,21]. The center of the white object was chosen as the point of the string, and it was tracked across all the video frames. This operation could be done for the next pixel bars and actually for all the points of the string. It should be noted that five videos were taken from each sample. The process of choosing the best video and the best point of the string is presented at the end of the flowchart. The difference between each pixel bar data in each video was calculated to select the best video; a video which has the slightest difference with the others is referred to as the selected video. The average coefficient of the variation between the pixel bars was calculated to choose the best point of the string, and a pixel bar with the lowest average coefficient of variation was selected. The string displacement was calculated from the difference in the pixels of the image and converted to a displacement in millimeters. Also, the number of the video frames was converted to time in seconds. Finally, a free decay was plotted for each sample. Basically, video processing data are recorded as a matrix

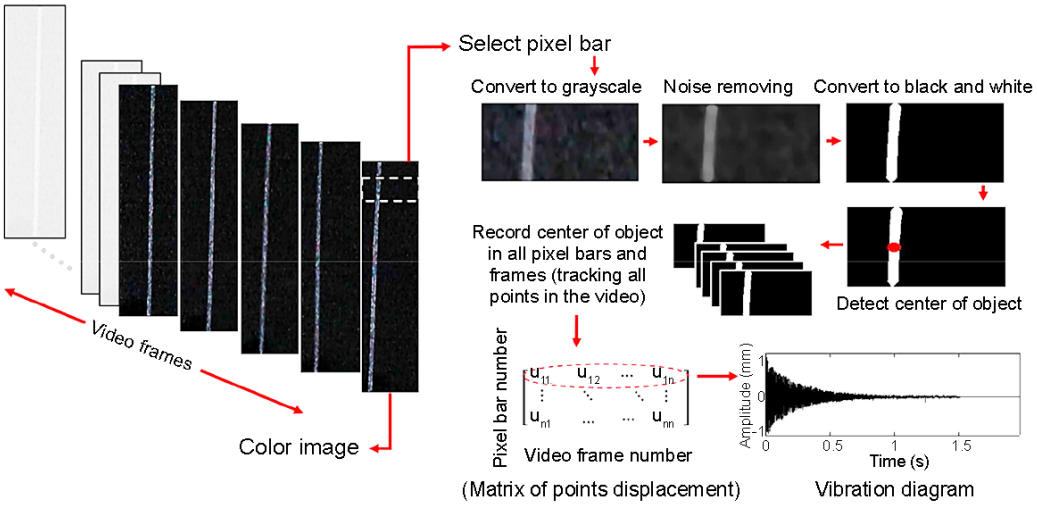

Fig. 6. Video processing for the free decay extraction.

array and a discrete signal. The discrete Fourier transform is one of the most important possible conversions to make on signals. The natural frequencies, amplitude, and phase can be determined with this conversion. In addition, logarithmic decrement is used to find the damping ratio of the free decays of string in the time domain. Besides, it is possible to compare video processing data with the results of theoretical models for plucked strings with viscous damping and obtain their vibrational properties such as damping coefficients.

III. RESULTS AND DISCUSSION

A. Video Processing Results

The vibration behavior of a string that was stimulated in the middle was recorded by the high-speed camera. The video processing method was used to track the movement of all the points in the string over successive video frames. The video processing is shown in Fig. 6.

A.1. Optimization of the Test Conditions Results

Three copper wires with different tensions of 20, 50, and 100 g and the excitation displacement of 4, 7, and 10 mm in the middle were tested to identify the best testing conditions. The free decays for the copper wire sample C-135 are presented in Fig. 7.

As the figure shows, in most cases, the free decays look like the superposition of two waves or more. This phenomenon may be related to the initial displacement and stimulation. It seems that the wires had a slight lateral movement perpendicular to the transverse vibration (i.e. in and out motion). This led to a combined response of lateral and transverse vibration. It occurred for all the three copper wires. So, it was decided that the initial displacement of the wires was reduced to remove this effect and decrease the lateral vibration. The vibration test was, thus, repeated for the 1 mm initial displacement. The free decays of the copper wire sample C-135 in 1 mm initial displacement and three tensions are presented in Fig. 8.

As shown in Fig. 8, it is clear that the effect of superposition has been reduced greatly due to a decrease in the excitation displacement. Through the repetition of the vibration test for the copper wires, it was indicated that 1 mm may be the best excitation distance for vibration tests and measurements with high speed cameras and video processing.

A.2. Monofilament Video Processing Results

According to the results of the copper wire vibration test, it was decided that the polypropylene monofilaments was tested in a condition in which the excitation distance was 1 mm and the weight was 20 g. These monofilaments had very low orientation because the speed of collecting them and the draw ratio after leaving the spinneret were very low. Using a great weight for the initial tension in the monofilaments would lead to excessive stretch and change in the linear density. So, it was decided to use the lowest weight of 20 g for the initial tension. Finally, the vibration test was done, the movement of the strings was recorded by the high-speed camera, and the vibrational diagram of one point of the monofilament string was plotted. The vibrational diagrams of the polypropylene monofilaments are presented in Fig. 9.

It can be seen that, as the linear density of the samples increases, the vibration frequency decreases, the amplitude increases, and the diagram is damped later. Therefore, the shape of the free decay of a string indicates that the data extracted from video processing can be useful for detecting the physical and apparent properties of that string. Using

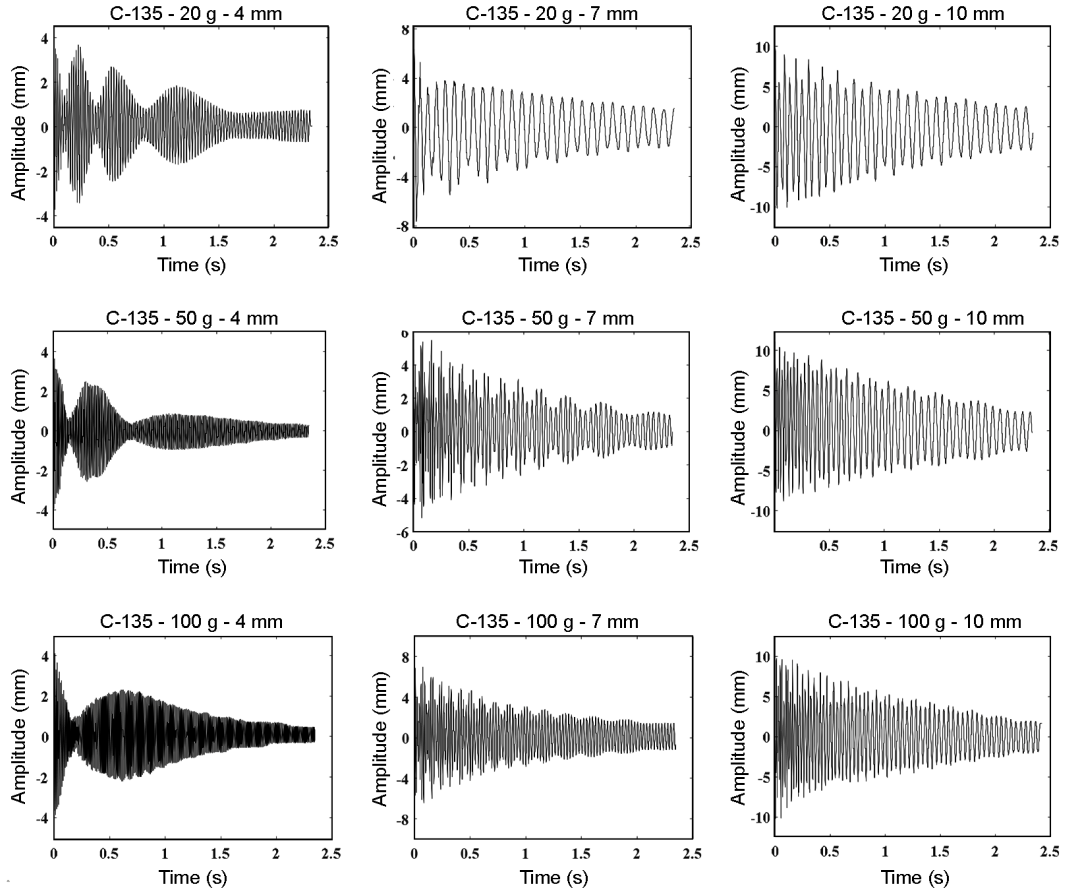

Fig. 7. Free decays for the copper wire sample C-135 at the distance of 4, 7, and 10 mm and the tension of 20, 50, and 100 g.

high-speed cameras may, thus, be a very simple way to measure the vibration behavior of strings and its relation with their linear density variation.

B. Vibration Information Result

B.1. Logarithmic Decrement Results

As shown in the diagrams of video processing, the vibration behavior of monofilaments is a damped sinusoid and the system exhibits a motion whose amplitude keeps diminishing. The decrease in amplitude from one cycle to the next depends on the amount of damping ratio. The ratio of any two successive amplitudes is constant and is a function of the damping only. The successive peak amplitudes bear a certain specific relationship involving the damping ratio, leading to the concept of logarithmic decrement. The logarithmic decrement and the damping coefficient for monofilaments obtained from Eq. (12) are given in Table II. As shown in Fig. 10, an increase in the monofilament linear density would cause a decrease in the damping coefficient.

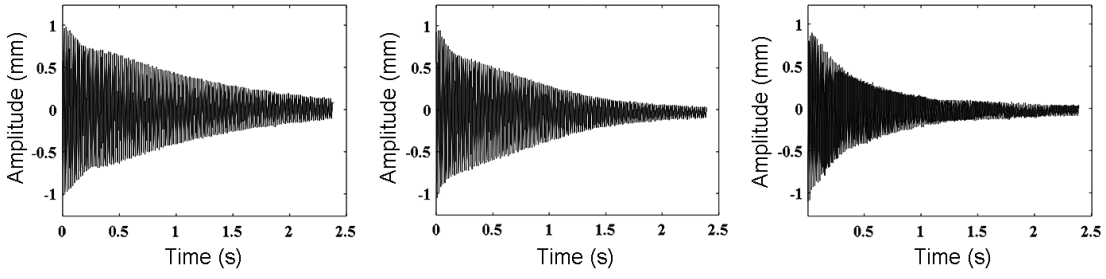

Fig. 8. Free decays for the copper wire sample C-135 at the distance of 1 mm and the tensions of: (a) 20 g, (b) 50 g, and (c) 100 g.

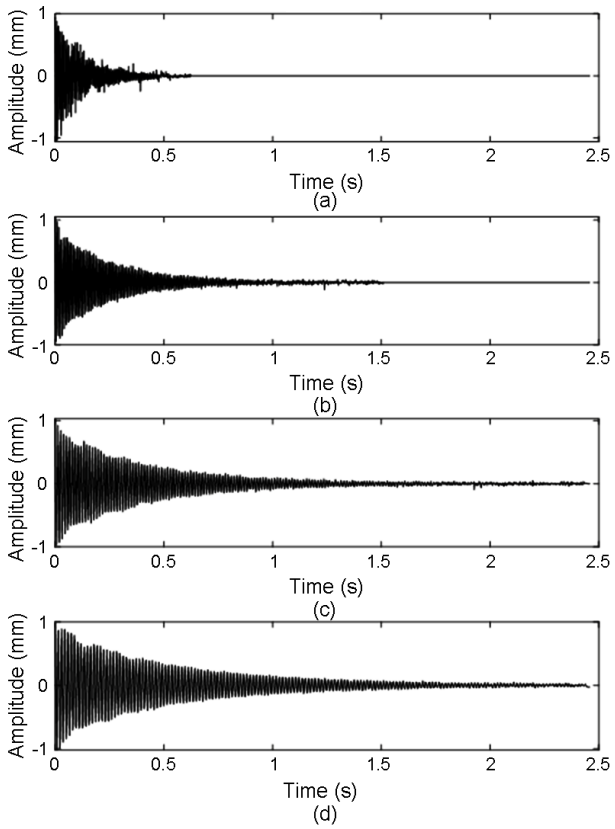

Fig. 9. Free decays of the polypropylene monofilaments taken through video processing: (a) P-120, (b) P-170, (c) P-220, and (d) P-290.

B.2. Fourier Transform Results

Generally, video processing data are recorded as a matrix array and discrete signals. The Fourier transform is one of the best conversions through which to obtain a content of such signals. The Fourier transform is useful for static signals in which the natural frequencies do not change over time. The signal in the Fourier transform is a mixed signal that has a domain and an angle at each point, or a frequency. The amplitude of the frequency is the effect of the specific frequency, and the angle of each point of the transformation is equal to the angle of the corresponding frequency. In this study, the Fourier transform frequency and the phase were obtained and plotted in separate graphs. As shown in Fig. 11, the specified peaks represent the participation of the natural frequencies with the respective amplitudes in each signal. The values of the highest amplitude at the natural frequencies are given in Table II. As shown in Fig. 12, it was also easy to track the angular values of the corresponding signal phase. The values of the phase are given in Table II. Thus, as shown in Fig. 10, once the linear density of a sample increases, the natural frequency decreases. The accuracy of these data was verified through a comparison of the results and the video processing diagrams (Fig. 9). It is expected that, when the frequency content of a signal is obtained by converting the Fourier series, the physical characteristics of monofilaments, such as their linear densities, can be compared.

B.3. Matching Theoretical and Experimental Results

The video processing results were compared with the theoretical model for the plucked string with viscous damping. The damping coefficient was selected as the optimization parameter. To optimize this parameter, the range of variation was considered as the maximum change that may occur due to an error in the measurement. The theory function was used as a standard to evaluate the accuracy of the model parameters when matching the experimental and theoretical results. This standard could, thus, be considered as the difference between the

TABLE II
VIBRATION INFORMATION OF POLYPROPYLENE MONOFILAMENTS

Methods	Parameters	P-120	P-170	P-220	P-290
Fourier transform	Frequency (Hz)	133.62	110.30	78.26	69.46
	Natural frequencies, ω_n (rad/s)	839.56	693.04	491.72	436.43
	Magnitude	4.65	3.32	4.85	6.42
	Phase, φ (rad)	0.46	0.86	0.75	0.90
Optimization (matching theoretical and experimental)	Natural frequencies, ω_n (rad/s)	916.72	615.63	514.22	352.61
	Damping coefficient, ζ	0.0078	0.0063	0.0041	0.0033
	Error (%)	23.7	16.9	21.7	14.9
Logarithmic decrement	Logarithmic decrement, δ	0.0611	0.0513	0.0430	0.0316
	Damping coefficient, ζ	0.0096	0.0082	0.0068	0.0050

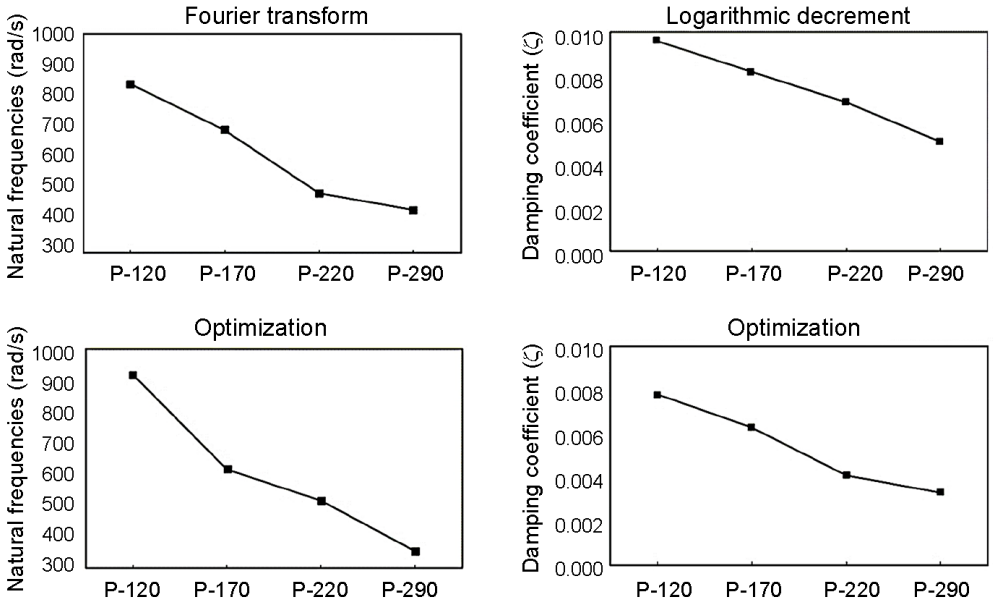

Fig. 10. Changing trends of the natural frequency and the damping coefficient in the Fourier transform, the logarithmic decrement and the optimization methods.

real model and the theoretical model. According to the equations given for a plucked string with viscous damping, the theory function was defined as Eq. (7). The process of optimizing the model parameters was similarly applied to all the sample strings through the error detection and correction technique, and the best values were determined for the damping coefficient and the natural frequency of the polypropylene monofilament. The best values of the damping coefficients and the natural frequencies obtained from the optimization are given in Table II. As the results showed, an increase in the monofilament linear density would cause a decrease in the damping coefficient and natural frequency. The theoretical diagrams derived from the model of the plucked string and the experimental diagrams are plotted in Fig. 13. It should be noted that the amplitude values have been normalized between zero and one. The agreement between the theory and the experimental data was excellent. This approach could validate the experimental results and successfully predict the vibration behavior of the textile filaments. So, it is easy to predict the trend of change in a physical parameter based on the trend of vibration parameters such as the damping coefficient.

IV. CONCLUSION

In this research, the vibration behavior of polypropylene monofilaments was evaluated using a high speed camera. The free decays were extracted by the video recordings of the string movements and video-processing algorithms. It was found that an increase in the linear density of the samples would cause a decrease in the vibration frequency and the free decay would also take longer to be damped.

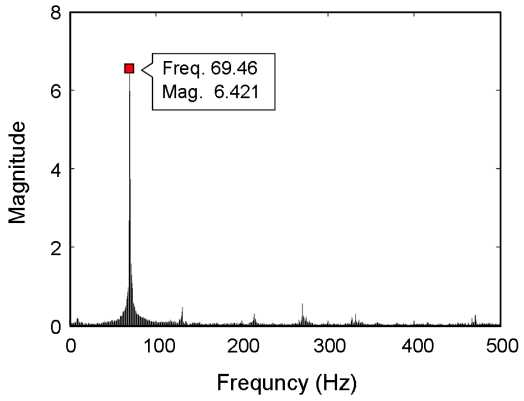

Fig. 11. Frequency-magnitude diagram for sample P-290.

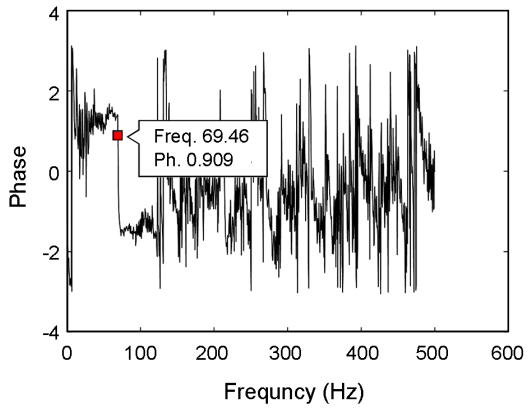

Fig. 12. Frequency-phase diagram for sample P-290.

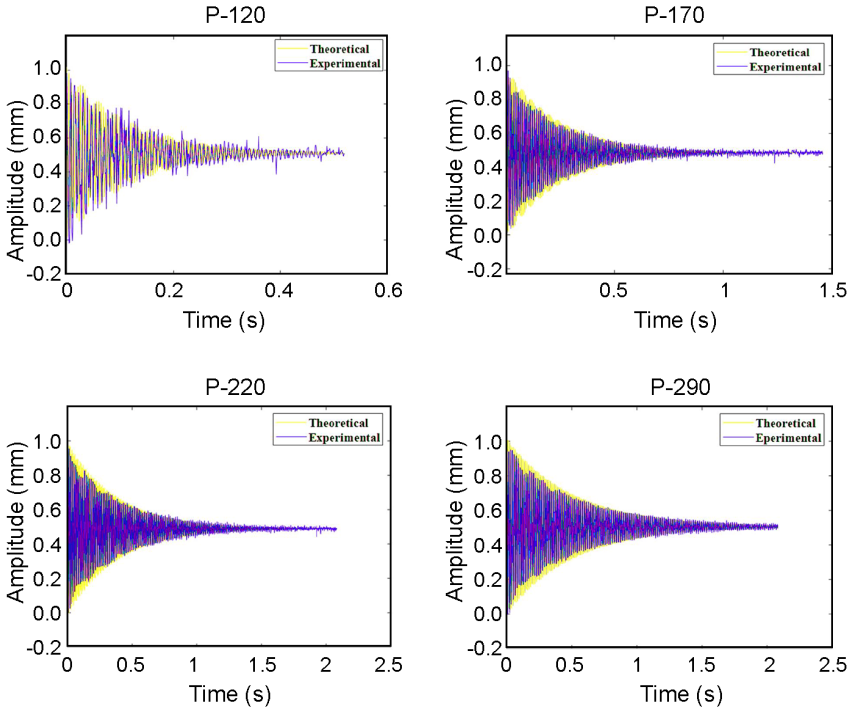

Fig. 13. Matching the experimental results (blue) and the theoretical results (yellow) based on the optimal damping coefficient.

The frequency content of the signals, such as the natural frequency, amplitude, and the phase, were calculated by the Fourier series. The logarithmic decrement and the damping coefficient for monofilaments were obtained. In addition, the results of the video processing were compared with those of a theoretical model for plucked strings with viscose damping and the optimal damping coefficient and the natural frequency were calculated. As the results indicated, an increase in the monofilament linear density would cause a decrease in the damping coefficient and its natural frequency decreases. So, the trend of changes in the physical properties of the monofilaments was easily predicted based on the trend of variation in the vibration parameters, such as damping coefficient and natural frequency. As a general conclusion, the data extracted from video processing are useful for determining the physical and apparent properties of textile strings. Also, high-speed cameras can serve as a very simple means of measuring the vibration behavior of textile strings and its relation with their linear density variation.

REFERENCES

[1] A. Askenfelt and E.V. Jansson, "From touch to string vibrations. III: String motion and spectra", *J. Acousti. Soc. Am.*, vol. 93, pp. 2181-2196, 1993.

[2] J. Pakarinen and M. Karjalainen, "An apparatus for measuring string vibration using electric field sensing", in *Proceedings of the Stockholm Music Acoustics Conference*, pp. 739-742, 2003.

[3] N. Plath, "High-speed camera displacement measurement (HCDM) technique of string vibration", in *Proceedings of the Stockholm Music Acoustics Conference,* pp. 188-192, 2013.

[4] J.G. Chen, N. Wadhwa, Y.-J. Cha, F. Durand, W.T. Freeman, and O. Buyukozturk, "Structural modal identification through high speed camera video: Motion magnification", in *Topics in Modal Analysis I*, Vol. 7, Ed: Springer, 2014, pp. 191-197.

[5] J. Kotus, P. Szczuko, M. Szczodrak, and A. Czyżewski, "Application of fast cameras to string vibrations recording", In: *2015 Signal Processing: Algorithms, Architectures, Arrangements, and Applications (SPA)*, 2015, pp. 104-109.

[6] M. Pàmies-Vilà, I.A. Kubilay, D. Kartofelev, M. Mustonen, A. Stulov, and V. Välimäki, "High-speed linecamera measurements of a vibrating string", In *Proceeding of the Baltic-Nordic Acoustic Meeting (BNAM)*, Tallinn, Estonia, 2014.

[7] D. Zhang, J. Guo, X. Lei, and C. Zhu, "A high-speed vision-based sensor for dynamic vibration analysis using fast motion extraction algorithms", *Sensors*, vol. 16, pp. 572, 2016.

[8] Z. Chen, X. Zhang, and S. Fatikow, "3D robust digital image correlation for vibration measurement", *Appl.*

Opt., vol. 55, pp. 1641-1648, 2016.

[9] M.N. Helfrick, C. Niezrecki, P. Avitabile, and T. Schmidt, "3D digital image correlation methods for full-field vibration measurement", *Mech. Syst. Signal Proc.*, vol. 25, pp. 917-927, 2011.

[10] J. Warburton, G. Lu, T. Buss, H. Docx, M.Y. Matveev, and I. Jones, "Digital image correlation vibrometry with low speed equipment", *Exp. Mech.*, vol. 56, pp. 1219-1230, 2016.

[11] X.P. Gao, Y.Z. Sun, Z. Meng, and Z.J. Sun, "On the transversal vibration of pile-yarn with time-dependent tension in tufting process", *Appl. Mech. Mater.*, vol. 29-32, pp. 1517-1523, 2010.

[12] X. Gao, Y. Sun, Z. Meng, and Z. Sun, "Analytical approach of mechanical behavior of carpet yarn by mechanical models", *Mater. Lett.*, vol. 65, pp. 2228-2230, 2011.

[13] D. Shen and G. Ye, "Study on the dynamic characteristics of warp in the process of weaving", *Fibers Text. East Eur.*, vol. 21, pp. 68-73, 2013.

[14] R.A. Malookani, S. Dehraj, and S.H. Sandilo, "Asymptotic approximations of the solution for a traveling string under boundary damping", *J. Appl. Comput. Mech.*, vol. 5, pp. 918-925, 2019.

[15] O. Serrano, R. Zaera, J. Fernández-Sáez, and M. Ruzzene, "Generalized continuum model for the analysis of nonlinear vibrations of taut strings with microstructure", *Int. J. Solids Struct.*, vol. 164, pp. 157-167, 2019.

[16] H. Zhang, C. Wang, and N. Challamel, "Modelling vibrating nano-strings by lattice, finite difference and Eringen's nonlocal models", *J. Sound Vib.*, vol. 425, pp. 41-52, 2018.

[17] M. Ferretti, G. Piccardo, F. dell'Isola, and A. Luongo, "Dynamics of taut strings undergoing large changes of tension caused by a force-driven traveling mass", *J. Sound Vib.*, vol. 458, pp. 320-333, 2019.

[18] A.W. Leissa and M.S. Qatu, *Vibrations of Continuous Systems*, USA: McGraw-Hill, 2011.

[19] W.J. Bottega, *Engineering Vibrations*, 2nd ed., USA: CRC, 2014.

[20] M. Emadi, M.A. Tavanaie, and P. Payvandy, "Measurement of the uniformity of thermally bonded points in polypropylene spunbonded non-wovens using image processing and its relationship with their tensile properties", *Autex Res. J.*, vol. 18, pp. 405-418, 2018.

[21] N. Dehghan, M.A. Tavanaie, and P. Payvandy, "Morphology study of nanofibers produced by extraction from polymer blend fibers using image processing", *Korean J. Chem. Eng.*, vol. 32, pp. 1928-1937, 2015.